Article

Not peer-reviewed version

Circular Management of *Lavandula stoechas* L. Post-Phytoremediation of Contaminated Soils: From Essential Oil to Biochar for Supercapacitors

María González-Morales , Natalia Díaz-Rodríguez , Luís Francisco Fernández-Pozo , María Ángeles Rodríguez-González *

Posted Date: 19 March 2026

doi: 10.20944/preprints202603.1522.v1

Keywords: circular economy; phytoremediation; *L. stoechas*; Metal(loid)s; distillation

 doi:10.20944/preprints202603.1522.v1

Article

Circular Management of *Lavandula stoechas* L. Post-Phytoremediation of Contaminated Soils: From Essential Oil to Biochar for Supercapacitors

María González-Morales [1], Natalia Díaz-Rodríguez [2], Luis Francisco Fernández-Pozo [1] and María Ángeles Rodríguez-González [1,*]

[1] Environmental Resources Analysis (ARAM) Research Group, University of Extremadura, 06006 Badajoz, Spain

[2] Department of Biochemistry and Molecular Biology and Genetics. University of Extremadura, 06006 Badajoz, Spain

* Correspondence: marodgon@unex.es

Abstract

This study proposes a circular economy model to manage plant residues derived from the phytoremediation of soils contaminated with heavy metals (Pb, Zn and Tl) by means of *Lavandula stoechas* L. Under greenhouse conditions, its effectiveness for phytostabilization was confirmed, as it retains most of the metals in its roots (65%) with bioconcentration factors less than one, confirming the suitability of the species for phytostabilization.The research focuses on the transformation of this waste into high value-added resources for various industries. In pharmaceutical and cosmetic applications, as essential oil and hydrosol were obtained through distillation with a yield of more than 0.4%. These products, rich in therapeutic terpenoids, are safe for public health as they are free of metal contaminants. Or in the energy sector, since the post-distillation residual biomass, which contains the metals retained in its tissues, was processed by pyrolysis to obtain biochar. This material achieved an electrical conductivity of 35 S/cm, demonstrating great potential for fabricating supercapacitor electrodes.In conclusion, this work validates the transition from hazardous waste to valuable industrial by-products, laying the foundations for its future implementation on an industrial scale under environmental safety criteria.

Keywords: circular economy; phytoremediation; *L. stoechas*; Metal(loid)s; distillation

1. Introduction

Mining activities are a powerful economic and social driver; however, they are also a significant source of waste generation, sometimes hazardous and toxic, as is the case of extraction of metallic minerals, where concentrations of up to 50 ppm can be found [1]. These wastes are the main source of toxicity and environmental pollution of anthropogenic origin [2]. In the European Union, these wastes account for more than 23% of the total waste generated [3].

Studies carried out in abandoned mining areas in the southwest of the Iberian Peninsula [4–7] have highlighted the severe impact of soil contamination on ecosystem services. Although the presence of heavy metals in the soil prevents may affect the colonization of certain plant species, there are native plants could develop ecophysiological responses to tolerate the stress caused by such pollution [8], assimilating heavy metals through their roots and accumulating them in their aerial or root tissues. If these heavy metals enter the food chain [9], detrimental effects on human health and ecosystems can occur [10].

Minimizing heavy metal contamination through phytoremediation techniques is very popular, (environmentally friendly, easy-to-apply and low-cost technology) because it allows to address the contamination of large land areas. Aromatic plants can play a crucial role, as they are inedible and

 doi:10.20944/preprints202603.1522.v1

do not facilitate the transfer of the heavy metals into the food chain, making them an excellent choice for long-term phytoremediation [11].

One of the most abundant plant species in the Mediterranean biogeographical region is *Lavandula stoechas* L. belonging to the Lamiaceae family and *Lavandula* genus [12]. This plant grows as a perennial, aromatic, and branched shrub that can reach up to one meter in height, with violet flowers arranged in spikes. It blooms in spring or early summer with dense and compact inflorescences [13]. Its presence has been described in soils highly contaminated with lead (Pb), zinc (Zn), and thallium (Tl) as a result of mining activities or diffuse pollution from coal combustion in thermal power plants [5]. This aromatic plant contains a large amount of essential oils and other secondary metabolites that make it suitable for gastronomic, cosmetic, and/or medicinal use [14].

The non-volatile compounds present in the essential oil extracted from *L. stoechas* make these species be considered as a source of phytochemicals with pharmacological interest with antioxidant, antimicrobial, anticancer, etc. properties [14]. Several ethnobotanical studies have shown the popular uses of some of these species for the treatment of digestion, headaches, heartburn, blood circulation, as a sedative, antidermatitic, nasal decongestive bronchitis, and asthma [15,16].

With the aim of following the principles of the Circular Green Economy, a deep research has been carried out focusing of on the use of the mining waste and plant biomass in the production of glass [17], new building materials [18] wastewater treatment [19] backfill in infrastructures [20], bioleaching as a means of mineral extraction [21] or in the encapsulation of toxic elements in cements, preventing their dispersion in the environment and allowing their disposal in controlled landfills or as construction materials after inerting [22]. Other authors state that both tailings and residual biomass after phytoremediation and/or distillation contain metals with potential for economic revaluation [23] and propose the conversion of this biomass into carbonaceous materials (biochar) by pyrolysis [24,25] for the synthesis of supercapacitor electrodes.

Supercapacitors are electrochemical energy storage devices that stand out for their ability to deliver a significant energy density without compromising high output power. The success of these systems lies in the use of carbon materials for the manufacture of their electrodes, as they offer high electrical conductivity, corrosion resistance, thermal stability and low production costs. In addition, its high surface area is essential to maximize the accumulation of electrical charge [26]. However, it has been proven that it is possible to further enhance its capacitance by incorporating multivalent cations from transition metals, when generating reversible redox processes [27].

This paper addresses the integral use (zero residue) of the aromatic plant L. stoechas found in a contaminated area around an abandoned Pb-Zn mine in the southwest of the Iberian Peninsula. After phytoremediation, it was used as a raw material to obtain essential oil (by steam distillation) and biochar (by pyrolysis). This is intended to integrate the principles of the ecological economy with the sustainable management of natural resources, and all this with a clear practical applicability within a sustainable business model with a positive environmental and economic impact. Both distillation compounds (essential oil and hydrolate) and biochar could be used in multiple applications.

The proposed application in this study for biochar is its use in supercapacitor electrodes, since there is some research suggesting that metal-contaminated plants after phytoremediation could increase the capacitance (cumulative charge) of supercapacitors [18,28,29].

The investigation of this work is innovative, because obtaining an environmental liability (*L. stoechas* plant contaminated after its use in phytoremediation) into an economic and social active (essential oils with multiple applications). In this way, it is possible to integrate the principles of ecological economics with the sustainable management of natural resources with clear practical applicability within a sustainable business model with a positive environmental and economic impact.

2. Materials and Methods

2.1. Phytoremediation Experiment

 doi:10.20944/preprints202603.1522.v1

2.1.1. Experimental Design

To evaluate the physiological response of *L. stoechas* to heavy metal stress, a potted trial was performed using a commercial substrate that was enriched with increasing concentrations of Pb (48, 60 and 1500 ppm), Zn (281, 351 and 700 ppm) and Tl (1, 1.25 and 700 ppm). These levels were categorized for each metal as minimum (A), medium (B), and maximum (C). The concentrations of Pb and Zn corresponding to level A (48 and 281 ppm, respectively) were established based on the safety thresholds defined by Spanish legislation (BOE-A-2005-895) that guarantee the safety of human health and ecosystems.

In the absence of specific limits in the State legislation for the case of Tl, the Canadian Guidelines for Environmental Quality (CCME, 1964) were taken as a reference, which establishes the safety limit value at 1ppm. In accordance with this standard, this concentration was established as minimum level A.

The maximum concentration (C) levels were determined based on the findings reported in a study conducted in an abandoned mining area [4,5], where concentrations of up to 1577 ppm of Pb, 716 ppm of Zn and 744 ppm of Tl were found, values that significantly exceed the maximum permissible concentrations (CMP) of the reference regulations. On the other hand, the mean concentrations (B) were established on a discretionary basis as intermediate values between levels A and C.

To evaluate the growth, accumulation capacity and distribution of heavy metals, an experiment was designed under greenhouse conditions using commercial seedlings of *L. stoechas*. The experimental design consisted of a total of 128 pots (11 cm in diameter and 8 cm in height), distributed in four blocks of 32 pots each. The control block was compared with the other 3, with three levels of treatment (A, B and C) with increasing concentrations of Pb, Zn and Tl. Pb and Zn were incorporated as nitrates (PbN_2O_6, $ZnN_2O_6{\cdot}6H_2O$), and Tl as sulphate (Tl_2SO_4). To ensure the homogeneity of the test, *L. stoechas* seedlings with uniform morphological characteristics (25 cm height and 5 roots) were used, grown in pots with a standard substrate load (750 g).

A universal substrate (COMPO SANA,® Germany) was used, where treatments A, B and C were integrated directly into the substrate. According to the data provided by the manufacturer, the chemical characteristics of the substrate used were as follows: slightly acidic pH (5-6.5 in $CaCl_2$), nitrogen content as N (200-450 ppm), phosphorus content as P_2O_3 (200-500 ppm) and potassium content as K_2O (300-550 ppm). The analysis of the substrate revealed very low levels of the heavy metals (loids) studied: Pb (0.01 ppm), Zn (1.60 ppm) and Tl (0.04 ppm).

For environmental control in greenhouses, the temperature was set at 22 °C and the relative humidity at 78%. The irrigation regime was established at three times a week or when the humidity of the substrate fell below 10%. This protocol was designed to simulate the historical rainfall (last 10 years) of the study area (Table 1). Irrigation was carried out with mains water early in the morning, proceeding to the collection of leachates at the end of the day.

Over a period of two months, biometric growth (length and biomass) of both the aerial and root systems was monitored weekly. Simultaneously, environmental variables and the total concentration of Pb, Zn and Tl in the substrate, leachate and plant tissues were recorded. Physiological parameters (chlorophyll content, photosynthetic rate, and transpiration) were measured every 12 hours; for this, a CCM-200 meter was used for chlorophyll and an LCi-BioScientific portable system for gas exchange.

All experiments were replicated 3 times picking 5 plants from each pot.

Table 1. Average monthly rainfall in the study area over the last 10 years [5].

Month	Ja	Feb	March	Apr	May	Jun	Jul	Aug	Sep	Oct	Nov	Dec
mL	187	224	268	268	121	41	13	11	121	227	293	211

2.2. Measurement of Metal Content

 doi:10.20944/preprints202603.1522.v1

The metal content (in substrate, plant, and leachate) was determined using ICP-MS with an Agilent Tech model 7900 instrument, after acid digestion (HNO_3 and HCl). A sample-to-extractant ratio of 1:10 was used [30].

2.3. Steam Distillation Experiment

The extraction yield for *L. stoechas* is very low [31], requiring at least 0.5 kg of plant material, but the biomass collected in the pots was not enough. For this reason, 3 kg of *L. stoechas* were collected near the tailings of an abandoned Pb-Zn mine located in the southwest of the Iberian Peninsula, which had been studied in previous works [5]. Once in the laboratory, the thicker stems were removed, and the leaves and flowers were reserved, washed with distilled water, and were left to air dry to remove excess moisture before proceeding with the essential oil extraction.

The distillation was carried out in a 12-liter capacity ALBRIGI In Hebra equipment, and each extraction was repeated 3 times. The extraction process was maintained for 60 minutes. The essential oil separation was carried out in a decanting funnel, and the oil was collected using a capillary pipette. The essential oils were immediately stored in 3 mL amber glass containers and refrigerated at 5ºC. The distilled plants were dried at 60ºC and ground for subsequent chemical analysis by ICP-MS, following the protocol described earlier.

The hydrolat (or floral water) obtained from the distillation was collected and analysed by ICP-MS to ensure the absence of heavy metals in its composition. The volatile components of the essential oils were determined by gas chromatography coupled to mass spectrometry (GC-MS) using an EVOQ-GCTQ PREM EO&CI system, with 0.5 µL injected.

The effectiveness of the distillation process was evaluated by calculating the yield (the ratio between the mass of the generated product and the plant used) for each experiment [32] using equation (1).

$$\text{Yield (\%)} = (M_1 / M_2) \times 100 \quad (1)$$

Where M_1 is the final mass of essential oil expressed in grams (g) and M_2 is the initial mass of plant material expressed in grams (g).

2.4. Statistical Analysis

All statistical analyses and graph generation were performed using IBM SPSS Statistics v.31 software. To verify the normality and homogeneity of the variables at the beginning and end of the trial, the Levene test was applied. The results indicated that no variable followed a normal distribution (Table S1, Supplementary Material). Consequently, box plots were used to visualize the dispersion of the data, facilitate comparison between groups and identify possible outliers (Figure S1-S2, Material Supplementary). Due to the nature of the results, Kruskal-Wallis tests were used to identify significant differences in the variables between the start and end of the experiment. Subsequently, Dunnett's post hoc T3 test was applied to determine which parameters, under the different concentrations of heavy metals, differed significantly from the control group (Tables S2-S6, Supplementary Material).

2.5. Biochar Synthesis

The distilled biomass was subjected to drying and milling processes prior to pyrolysis. It is important to know the pyrolysis temperature to complete conversion of the distilled biomass into stable carbonaceous material, since incomplete carbonization would be inefficient for its application in supercapacitors, since the remaining organic matter would reduce the performance of the electrode and present low chemical stability, easily degrading in basic electrolytic media an DTA-TG analysis was previously performed in a nitrogen atmosphere (100mL/min). Since no weight loss was observed after 600 °C, pyrolysis was carried out at this temperature (600 °C), in a tube furnace (nitrogen atmosphere, 4 hours of dwell time, gas flow of 100 mL/min). The resulting biochar was structurally and texturally characterized to verify its thermal stability and porosity. DTA-TG (TA instruments

 doi:10.20944/preprints202603.1522.v1

analyser, model Q600), Infrared spectroscopy (Perkin Elmer BXII spectrophotometer) and Raman spectroscopy (Renishaw inVia spectrophotometer) and nitrogen adsorption (Micromeritics Tristar 3000) were used. Finally, the carbon and nitrogen content was determined by elemental analysis (LECO CS200, LECO TC500).

3. Results and Discussion

3.1. Morphometry

The degree of plant damage when exposed to various concentrations of heavy metal(loid)s (Pb, Zn, and Tl) was studied through the evolution of greenhouse plants during the 8 weeks of the experiment. Figure 1 shows data on plant length (root and aerial parts), weight, and some physiological parameters such as chlorophyll content, photosynthetic activity, and transpiration rate.

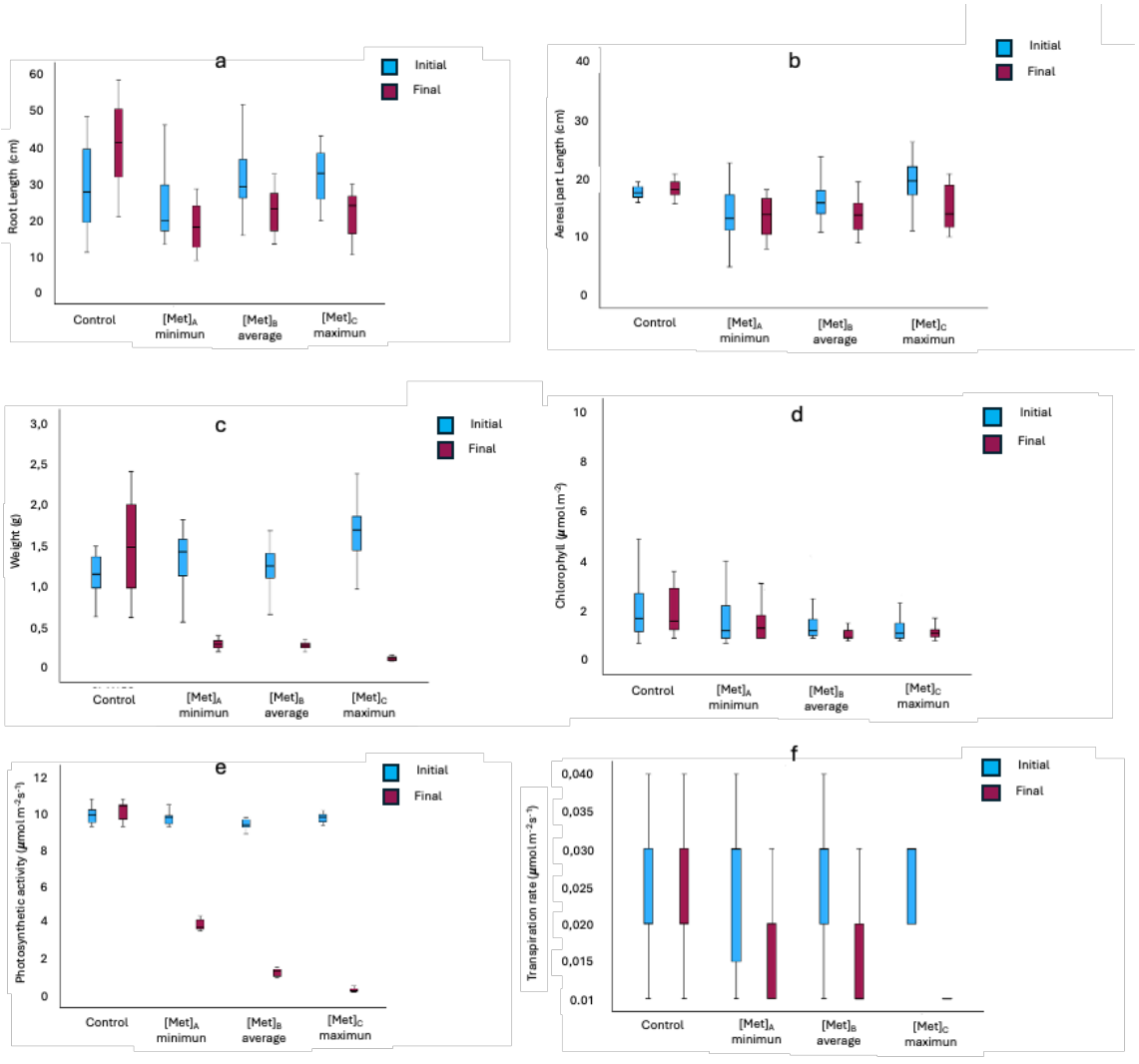

Figure 1. Evolution of the morphological characteristics studied in *L. stoechas* in the presence of metal(loid)s.

It is observed that the presence of metal(loid)s inhibits the metabolism of the seedlings, thus affecting their growth, both in terms of the root size (Figure 1a) and the aerial part (Figure 1b). Nevertheless, *L. stoechas* grows and develops under all the experimental conditions, even when the concentrations of metal(loid)s are very high (maximum concentration C), demonstrating its adaptability to certain levels of contamination. Photosynthetic activity (Figure 1e) and transpiration rate (Figure 1f) decrease significantly, which also affects biomass accumulation and leaf firmness. However, no clear loss of vitality or wilting was observed in any of the pots during the experiment.

 doi:10.20944/preprints202603.1522.v1

Similar behaviours have been described by various authors [33,34] who observed changes in the physiology of rice seedlings subjected to Pb and Cd stress. However, others [35], when analysing *Dittrichia viscosa* leaves cultivated in an antimony-rich substrate, found no significant oxidative damage or differences in photosynthetic parameters, which they attributed to the plant's adaptation to antimony stress.

Statistical analysis of the results provided information on the truly significant changes ($p<0.01$) in the growth and physiology of *L. stoechas*. Table S7 Supplementary Material presents the significantly relevant characteristics. As expected, the most significant changes in the morphological characteristics of the plant take place with the maximum concentrations of pollutant metal(loid) added (C treatment), especially in weight, photosynthetic activity and transpiration rate. Due to that the concentrations of added metal(loid)s in treatments A and B are close (48-60 ppm for Pb; 281-351 ppm for Zn and 1-1.25 ppm for Tl), in these treatments no very significant differences are observed. On the other hand, the morphology of this plant is clearly affected even with small concentrations of metal(loid)s, much lower than those found in the reference area of this study [5].

Post hoc tests (Tables S2-S6, Supplementary Material) confirmed the initial observations, indicating that there were no significant differences in root and aerial parts length between treatments B and C, so the plant is able to tolerate a minimum concentration of metal(oid)s for which the morphology of the plant is not affected. Regarding plant weight, post hoc tests does not show significant differences between all treatments. The differences between the initial and final weights are very high, indicating that the plant is affected significantly with the concentration of metal(loid)s.

With respect to physiological parameters—chlorophyll content, photosynthetic activity, and transpiration rate—no significant differences were detected among the different treatments, although differences were found between each treatment and the control. A more specific study on the effects of high levels of heavy metal contamination would be of great interest to further clarify these findings.

On the other hand, related to the accumulation of the contaminants in the roots, aerial parts, retained soil and leachates showed significant differences between the control pots and those pots subjected to treatments as expected. In particular, no significant differences were found between treatments A and B for the heavy metals analysed in the aerial parts. A similar pattern was observed in the leachates, where no significant differences were found between A and B in the case of Zn and Pb. This same trend was also observed in the heavy metal(loid)s content present in the soil.

3.2. Study of Heavy Metal(loid)s Content

In Table 2, the concentrations (%) extracted by the plant at each of the dosages are shown. It is observed that the metal(loid)s remains retained in the soil, especially Zn, and that regardless of the metal(loid) considered, all of them accumulate preferentially in the root, which is associated with the mechanism of heavy metal uptake. Pb is typically absorbed through non-metabolic or passive processes, while Zn is actively absorbed through a metabolic process [36]. However, *L. stoechas* demonstrates great phytoremediation potential for this metal(loid)s, especially for Pb and Tl, extracting more than 30% of the initial content added to the pots.

The contents of Pb, Zn, and Tl found in the leachates at the end of the experiment indicate the existence of mobile forms, despite the low acidity of the soil. Thallium and zinc are the predominant elements in these leachates, with Tl being more favourable, indicating greater solubility of these elements. Although the washing conditions in the experiments were intense, the decreasing concentrations found for Zn and Pb suggest difficulties in the availability and transport of these metals to areas farther from the contamination source, minimizing the potential environmental impact.

Table 2. Pb, Zn and Tl contents (%) in soil, vegetation and leachate after the study. Treatment A: minimum metal concentration; Treatment B: average metal concentration; Treatment C: maximum metal concentration.

Metal	Initial soil dosage (ppm)	Final soil (%)	Root (%)	Aerial (%)	Leachate (%)

 doi:10.20944/preprints202603.1522.v1

Control	Pb	0.01	100	0	0	0
	Zn	1.60	25.62	28.12	38.12	8.12
	Tl	0.04	25	0	75	0.00
A	Pb	48.18	68.34	26.38	4.98	0.29
	Zn	281.34	76.80	13.72	8.80	0.67
	Tl	1	70	14	16	0
B	Pb	60.26	67.59	28.11	4.14	0.15
	Zn	352.79	79	14.45	0.06	0.57
	Tl	1.25	65.60	21.60	12.00	0.80
C	Pb	1500.43	68.13	16.89	14.88	0.11
	Zn	706.61	85.92	9.75	3.86	0.46
	Tl	700.62	70.37	17.61	11.05	0.97

The retention of Pb, Zn, and Tl in the soil was significant ($p<0.01$) for all treatments (A, B, and C).

The bioconcentration factor (BAF), calculated as the ratio between the metal(loid) concentration in the plant (root and aerial parts) and its total concentration in the soil, is shown in Table 4. The total amount of each metal was considered as the sum of the metal content in the soil plus the content in the leachate. In all treatments, values less than one were obtained, indicating that *L. stoechas* behaves as an excluder species, with a low capacity to accumulate Pb, Zn, and/or Tl in its tissues. Similar behaviour of this plant has been reported by other authors for metals such as Pb and Hg [36,37] or for Zn [38].

The translocation factor (TF), calculated as the ratio between metal concentrations in the aerial part and in the root (Table 3), is less than 1 in all cases, indicating that *L. stoechas* does not transport metals to the aerial part, behaving as a non-accumulator species. Similar results were obtained with *L. pedunculata* for Pb and Zn in the southwest of the Iberian Peninsula [37]. However, *L. vera* was found to accumulate metals in the aerial part [39] for Pb and to a lesser extent for Zn, which is attributed to the fact that plants grown in pots are more exposed to the heavy metal than those grown in the field, due to their more developed root system.

Given its phytostabilizing potential, *L. stoechas* it is considered suitable for immobilizing contaminants in the soil, particularly Pb, Zn, and Tl, thus preventing the spread of contamination to surrounding areas. In areas contaminated by metal(loid)s, agricultural or livestock activities cannot be carried out, to avoid the potential risk of food produced containing soil contamination (even at trace levels). Therefore, this study proposes the utilization of this plant, so that after its use in phytoremediation, an added value could be obtained from the distillation byproducts, as it is an aromatic plant from which essential oils could be extracted.

Table 3. Bioconcentration and translocation factor. Treatment A: minimum metal concentration; Treatment B: average metal concentration; Treatment C: maximum metal concentration.

	Metal	**BAF**	**FT**	**Final soil**	**Root**	**Aerial**
						(ppm)
A	Pb	0.38±0.08	0.19±0.06	32.93±4.25	12.71±1.25	2.40±0.32
	Zn	0.18±0.02	0.64±0.10	216.08±25.30	38.60±4.12	24.76±4.17
	Tl	0.20±0.03	0.94±0.20	0.7±0.06	0.14±0.01	0.16±0.01
B	Pb	0.42±0.12	0.15±0.05	40.73±15.23	16.94±1.23	2.5±0.02
	Zn	0.18±0.06	0.41±0.15	278.72±29.28	51.01±8.84	21.04±1.96
	Tl	0.33±0.08	0.55±0.15	0.82±0.06	0.27±0.01	0.15±0.01
C	Pb	0.25±0.02	0.88±0.20	1022.21±133.87	253.4±33.66	223.22±18.84
	Zn	0.11±0.01	0.39±0.10	607.14±45.23	68.93±9.47	27.26±3.42
	Tl	0.25±0.02	0.63±0.17	493.01±39.39	123.41±9.87	77.42±9.63

 doi:10.20944/preprints202603.1522.v1

3.3. Essential Oil Extraction

Data on the performance of the extraction process, calculated using equation [1], are shown in Table 4, together with data on the distilled plant biomass and the amount of essential oil obtained in each extraction. The density of the oil, calculated by pycnometer, was 0.93 g mL^{-1}. Although the yields obtained may seem low compared to those of other *Lavandula* ssp. [31], are expected at the laboratory scale for *L. stoechas* [40].

Table 4. Yield data of the extraction process.

Extraction	Biomass (g)	Essential oil (mL)	Yield (%)
1	589.88	3.00	0.47
2	434.75	1.96	0.42
3	489.98	2.00	0.38

The quality of the essential oil obtained was reflected in its sensory profile, showing great transparency as well as an intensely floral, slightly herbaceous, and quite refreshing aroma. These properties are highly appreciated in aromatherapy applications, as they provide sedative and anxiolytic effects [41].

Through gas chromatography, more than 40 components were identified in the essential oil of *L. stoechas*, with around 20 of them presenting relative concentrations greater than 1%. Figure 2 shows one of the chromatograms obtained. The predominant components include monoterpenes (α-pinene, limonene, camphene), some sesquiterpenes (cubenol), ketones (camphor, fenchone), alcohols (linalool, borneol, cubenol), esters (linalyl acetate, bornyl acetate), and oxides (1,8-cineole or eucalyptol). All these terpenes have demonstrated therapeutic effects due to their analgesic, anti-inflammatory, or anxiolytic functions [42]. They combat depression and anxiety, can be considered anticancer agents [43], and fight fungal and bacterial infections [44]. This therapeutic effect may be due to the synergy of all these components or the action of one of them in particular. For example, sedative action is attributed to linalool and linalyl acetate, and antimicrobial action to linalool, 1,8-cineole, camphor, terpineol, and α-pinene [45].

The low proportion of linalool and linalyl acetate in this oil reduces the potential toxicity that high percentages of these compounds confer to the oil, according to literature where studies on the genotoxicity evaluation of lavender essential oils in humans have been conducted [46].

 doi:10.20944/preprints202603.1522.v1

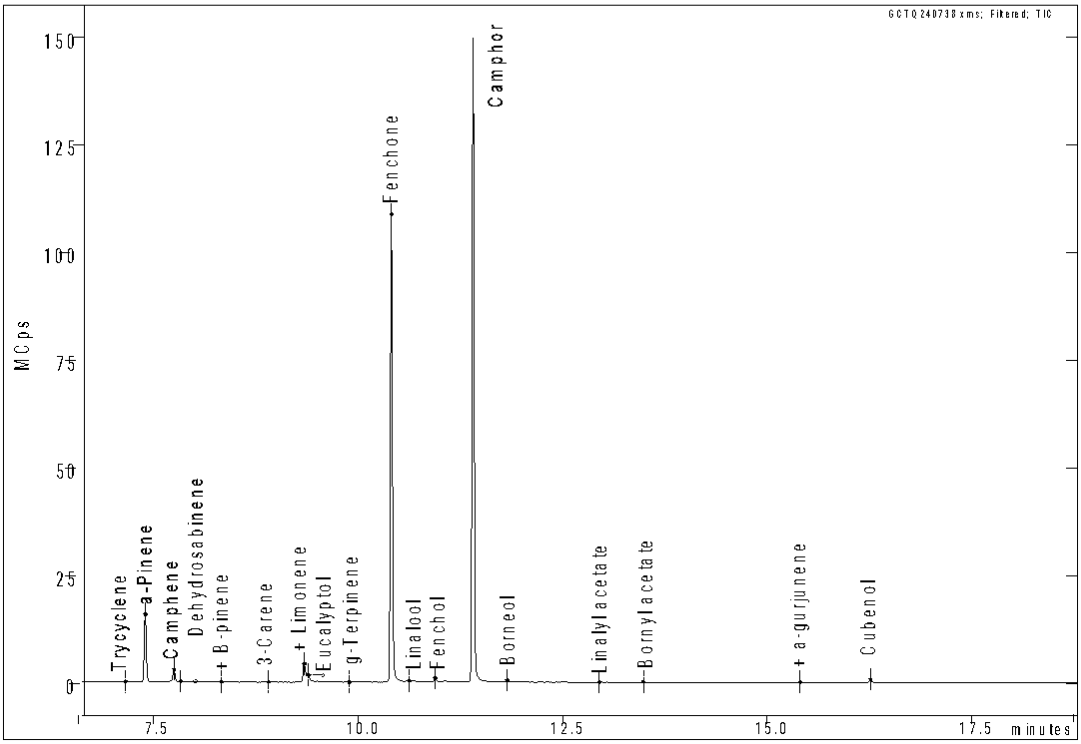

Figure 2. Chromatogram of *L. stoechas* essential oil.

Table 5 presents the Pb and Zn contents in the distillation products (essential oil, hydrolat, distilled biomass, distillation wastewater). Also included in this table is the initial metal concentration in the soil and plant before extraction.

Table 5. Pb and Zn concentration in the soil and plant from the mine, and in the distillation by-products (hydrolat, distilled biomass, distillation wastewater).

	Pb (ppm)	**Zn (ppm)**	**Tl (ppm)**
Essential oil	n.d.	n.d.	n.d.
Hydrolat	n.d.	n.d.	n.d.
Biomass after distillation	173±14	307±11	195±15
Residual water after distillation	0.02±0.01	0.96 ±0.04	0.04±0.02
Mine soil	254.6±183.6	367.4±212.4	314.9±95.4
L. stoechas mine (leaves and flower)	185.3±92.8	339.8±141.7	216.0±85.1

As the metals are not transferred to either the essential oil or the hydrolat (Table 6), both could be uses in the said applications (cosmetics, pharmaceuticals, emotional wellness, etc.). The hydrolat (floral water) is a highly valued product in cosmetic applications, as it has a mild lavender aroma and can be used in the production of soaps, facial toners, or creams, even when derived from plants with high levels of heavy metals, as is the case in this study.

Although studies on the extraction of essential oil from *L. stoechas* phytoremediation residues are scarce, various authors have observed the absence of heavy metals in the essential oil of mint and basil grown in contaminated soils [47] or in lemongrass [48]. Angelova et al. [39] reported that in soils

 doi:10.20944/preprints202603.1522.v1

contaminated with Pb and Zn in Bulgaria, the essential oil of *L. vera* showed no traces of these metal(loid)s. Similar results to those obtained in this study were found in a study by Sierra et al. [36] for *L. stoechas* plants grown in Hg-contaminated soils in the Iberian Peninsula.

3.4. Biochar Characterization

Figure 3 shows the DTA-TG for the distilled plant. The endothermic peak centered above 80ºC leads to a weight loss of 7%, and is attributed to the dehydration of the sample. Afterwards, four stages of weight loss are observed located at 270, 360, 430, and 600ºC, corresponding to the thermal decomposition and carbonization of the components of the plant matter; hemicellulose (170-280ºC, 23.54%), cellulose (280-380ºC, 29.56%) and lignin (> 380ºC, 18.6%) [49].

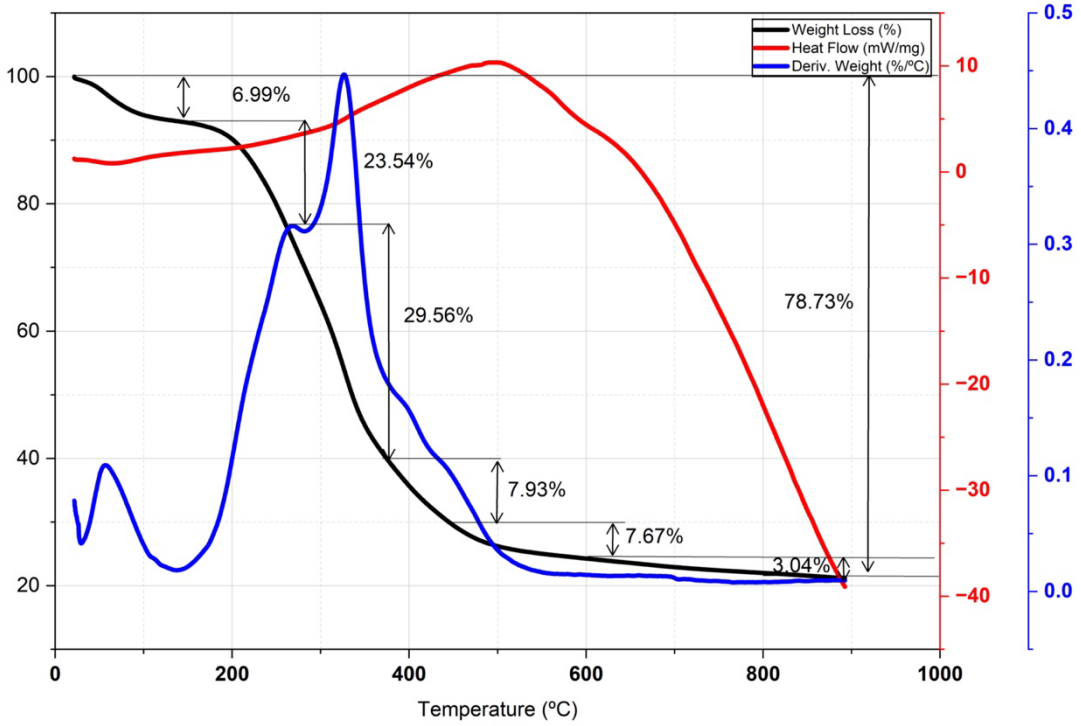

Figure 3. DTA-TG registration of distilled biomass in an inert atmosphere (N_2).

3.4.1. Textural Characterization of Biochar (N_2 Adsorption)

The textural characterization of the biochar was carried out by nitrogen physisorption at 77 K. Prior to the analysis, the sample was subjected to a degassing process at 150 °C under nitrogen flux for 18 hours to eliminate species adsorbed or occluded in the pores (CO_2 and water vapor). The resulting adsorption-desorption isotherm (Figure 4) is classified as type IV with a hysteresis cycle, which is characteristic of mesoporous solids according to IUPAC [50]. The hysteresis cycle observed in the relative pressure range P/P0 from 0.4 to 0.8 confirms the presence of mesopores, while the notable increase in the volume adsorbed of nitrogen at low pressures (P/P0< 0.01) probably indicates the coexistence of a network of micropores.

 doi:10.20944/preprints202603.1522.v1

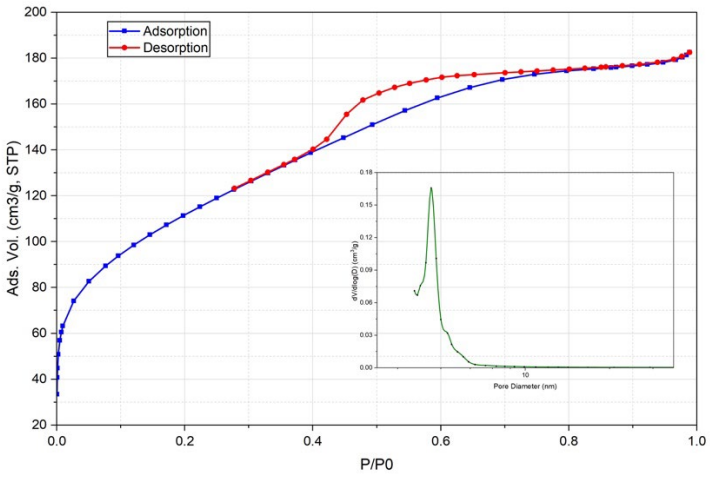

Figure 4. Adsorption-desorption isotherm and pore diameter of the biochar.

The BET model was used for obtaining the specific surface area (SSA), using the Brunauer-Emmett-Teller equation (BET)[51], applied in the relative pressure range ($0.05 \leq P/P0 \leq 0.3$) where the model presents higher linearity. The biochar presented a SSA of 393.7 m^2/g.

The pore size distribution of biochar was determined from the desorption curve of the isotherm using the BJH method [52] as it is shown in Figure 4 inside. This material presents a trimodal porosity profile, with maximum peaks centered at 3.1, 3.6 and 4.5 nm in diameter. The marked increase of the curve in the region of lower diameters suggests the presence of micropores, while the stabilization of the curve towards larger diameters confirms the absence of significant macroporosity.

By mathematical integration of the pore distribution curve (Figure 4), the contribution of the mesopores to the total SSA is 158.8 m^2/g. Since the total SSA is defined as the sum of the meso and micropore contributions ($SSA_{BET} = SSA_{micropores} + SSA_{mesopores}$), the surface area associated with the micropores was calculated by difference, resulting in a value of 234.9 m^2/g. Then, the ratio of micropores to mesopores is approximately 60/40, indicating that biochar has a predominantly microporous nature.

3.4.2. Thermal Characterization (Atd-Tg)

The final biochar was also characterized by DTA-TG in air atmosphere to evaluate its thermal stability and quantify the carbon content after pyrolysis as shown in Figure 5. The DTA curve presents four stages of mass loss. The first stage (20-200 °C, 4.5%) corresponds to the desorption of adsorbed hygroscopic water. The main event occurs between 200-580 °C, with a 75% loss attributable to carbon combustion. This process is divided into two stages: the oxidation of carbon derived from hemicellulose and cellulose (54.99%) and, subsequently, that of carbon from lignin (20%). These results are consistent with the characterization of the raw material (Figure 3), which reported a hemicellulose and cellulose content close to 50%. Finally, the peak at 640 °C is associated with the combustion of carbon fractions with a higher degree of crystallinity, confirming that the thermal stability of biochar is intrinsically linked to the organic structure of the plant precursor.

 doi:10.20944/preprints202603.1522.v1

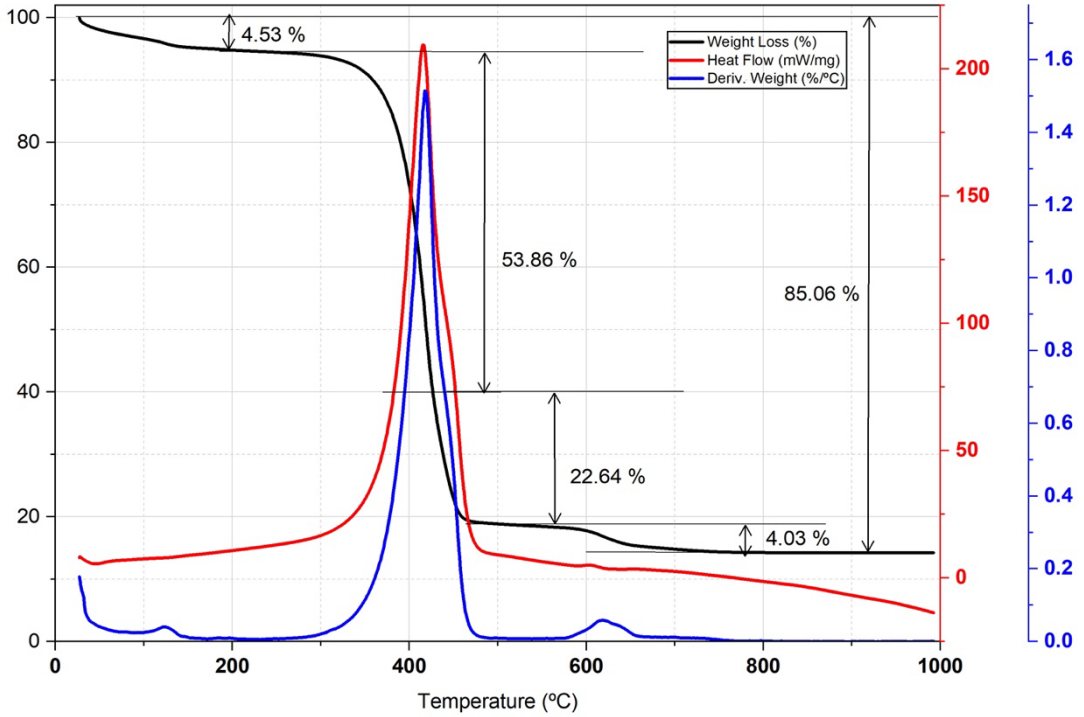

Figure 5. DTA-TG Registration of Biochar Sample in Air Atmosphere.

3.4.3. Structural Characterization

3.4.3.1. Infrared Spectroscopy

In order to understand the difference between carbon and the obtained biochar, Figure 6 shows the FT-IR (ATR) spectra of both materials. While pure carbon does not show any signals, the presence of vibrational bands in the region of 1500-600 cm^{-1} in the biochar evidences the existence of the other components than elemental carbon. These results confirm the presence of inorganic matter after the pyrolysis process, consistent with the DTA-TG analyses reported by Li & Chen [53].

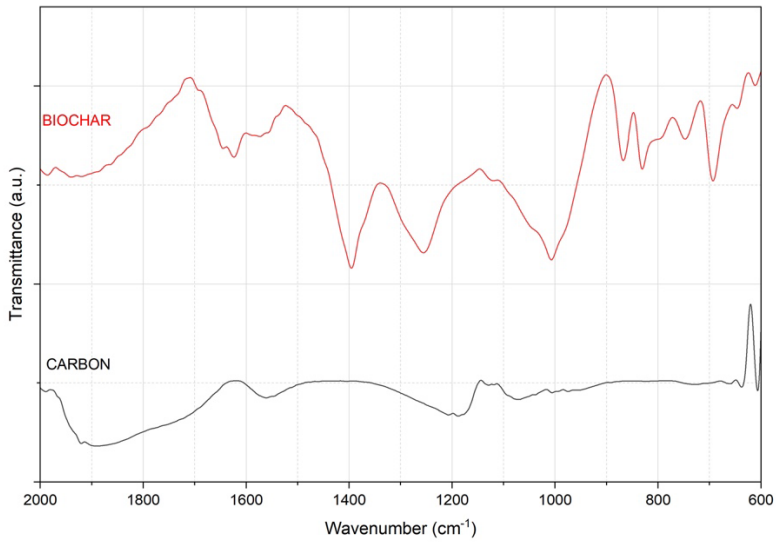

Figure 6. IR spectrum of the biochar obtained.

 doi:10.20944/preprints202603.1522.v1

To quantify the total carbon of the biochar a combustion process was performed at 1000 °C for 4 hours. This process transforms carbon into CO_2 and isolates the inorganic fraction (ash). The analysis of these ashes by IR spectroscopy (Figure 7) revealed characteristic bands of silicon (1094 and 1017 cm^{-1}), calcium (885 cm^{-1}) and manganese (932 cm^{-1}) oxides, results that are consistent with the XRF and XRD analysis shown in Table 6.

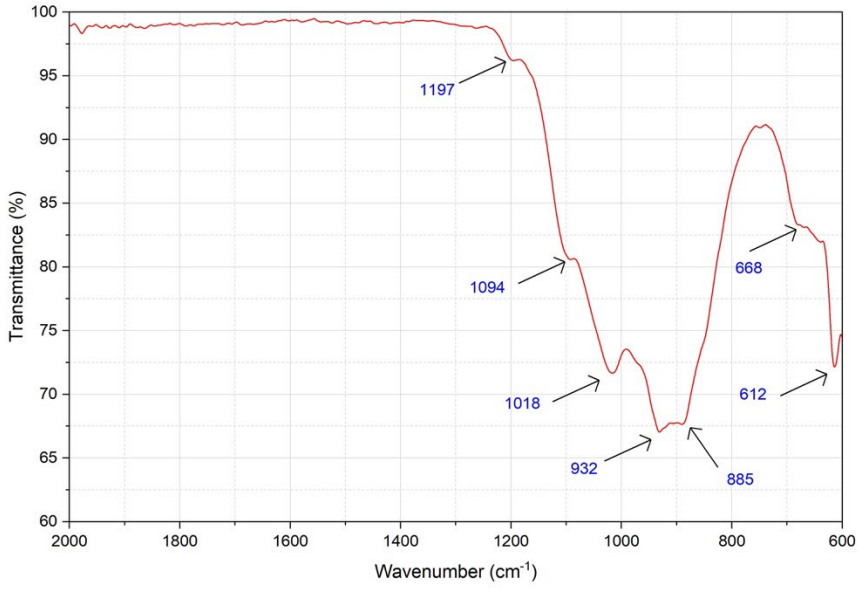

Figure 7. Infrared spectrum of biochar burned at 1000ºC.

Table 6. Chemical composition of the residue of the burned biochar.

	Al_2O_3	SiO_2	Fe_2O_3	CaO	K_2O	ZnO	SrO	Na_2O	P_2O_5	MgO	TiO_2	Pb_2O_3	MnO	SO_3
LMA %	6.5	25.8	2.30	31.1	10.3	0.30	0.33	2.41	5.64	10.2	036	0,003	0.31	4.26

3.4.3.2. Raman Spectroscopy

The Raman spectrum of biochar (Figure 8) presents the distinctive bands of carbonaceous materials. The D band at 1340 cm^{-1} is identified, caused by disorder in the graphitic structures, and the G band at 1590 cm^{-1}, associated with the energy of the sp^2 bonds and the presence of ordered graphitic domains [54].

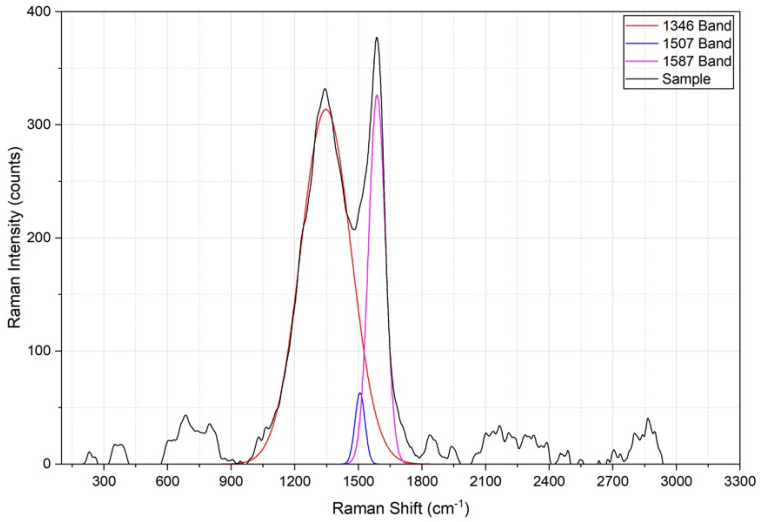

 doi:10.20944/preprints202603.1522.v1

Figure 8. Gaussian deconvolution of the Raman spectrum of biochar.

After the deconvolution of the experimental spectrum, an additional band (D') is identified at about 1500 cm^{-1}. Although its intensity is moderate, this signal confirms the coexistence of amorphous carbon in the sample (1490 cm^{-1}).

3.4.3.3. Chemical Characterization (Elemental)

The biochar obtained by pyrolysis of lavender biomass (stems, leaves and flowers) presents a predominantly carbonaceous composition with a majority carbon content (68.2%). The remaining mass balance (13.4% oxygen and an elemental total of 83.12%) suggests that, together with the organic structural polymers (cellulose, hemicellulose and lignin), inorganic components coexist in the form of metal oxides (Si, Ca, Mn, Ti, etc.). These values are (68% C, 0% S, 1,52% N and 13,4% O).

3.5. Application of Biochar in Electrodes

The performance of energy storage systems is conditioned by the properties of their electrodes [55]. However, the disordered structure often exhibited by conventional carbon materials limits electrical conductivity, and rarely combines high conductivity with high porosity [56].

Although elemental analysis shows a limited purity (68.2%) and moderate specific surface area (393.7 m^2/g) compared to activated or graphene-doped carbons [57], the material obtained by pyrolysis of the distilled plant has an acceptable porous structure due to its mesopores and micropore content. It should be noted that, according to [58], an increase in the specific surface area does not guarantee a greater storage capacity, since the size and distribution of the pores play a more decisive role.

To overcome the limitation of low charge density in supercapacitors, it is common to incorporate polyvalent metal oxides that facilitate faradaic redox reactions, which are the ones that determine the accumulation of electric charge [59]. In our study, biochar already possesses these properties intrinsically since the plant naturally bioaccumulated polyvalent metals (Pb, Zn, Ti, Cu and Fe) in its tissues as confirmed by the ICP-MS analysis. These elements not only promote charge accumulation but are probably responsible for the material's remarkable electrical conductivity (35 S/cm). This result supports the need to study the analysis of the electrochemical performance (capacitance) of the obtained biochar, as well as to investigate other methods to optimize its porosity and specific surface.

4. Conclusions

Lavandula stoechas L. stands out for its ability to grow in contaminated soils, which makes it a plant with phytoremediating potential. This species tends to accumulate heavy metals mainly in its roots, making it difficult to move them to aerial parts, which limits the transfer of these pollutants to the food chain. However, changes in soil pH can increase the mobility of metals and facilitate their release into the environment, with the consequent risk of dissemination to terrestrial or aquatic ecosystems. It is therefore crucial to remove plants after the decontamination phase, as they become hazardous waste due to their metal content.

This study proposes a sustainable alternative for the comprehensive management of *L. stoechas* waste contaminated with heavy metals, while promoting its revaluation in the form of by-products with therapeutic and cosmetic and electric applications, without representing any risk to human health.

The valorization of this aromatic plant through the extraction of essential oils, safe for use in medicine and cosmetics, offers an effective way to prevent the release of metals into the environment. Thus, it contributes not only to the ecological recovery of areas affected by mining activities, but also to the promotion of circular economy and more sustainable management of plant waste.

 doi:10.20944/preprints202603.1522.v1

After optimizing this process, the safety of the products was confirmed, since contaminants are not transferred to the essential oil or hydrolate. This guarantee of safety for human health made it possible to move towards practical application, the production of soaps.

In addition, since heavy metals remain immobilized in plant waste after distillation, these could be used in the production of biochar with stabilizing properties, aligning with the "zero waste" objective, fundamental in the framework of the circular economy.

The characterization of the vegetal biomass material, composed mainly of cellulose, hemicellulose and lignin, presented mainly an amorphous structure with low thermal stability, which reaches complete carbonization at 600 °C. Although biochar has a moderate specific surface area (393.7 m^2/g), its structural properties make a suitable candidate to modify its surface. These treatments would optimize the porosity expanding its possibilities of technological use.

Supplementary Materials: The following supporting information can be downloaded at the website of this paper posted on Preprints.org.

Author Contributions: María González-Morales: Investigation, Writing and review; Natalia Díaz-Rodríguez: Investigation, Review and editing; Luis Francisco Fernández-Pozo: Conceptualization, Data curation, Investigation, Methodology, Supervision, Writing-review and editing; Mª Ángeles Rodríguez-González: Conceptualization, Data curation, Funding acquisition, Investigation, Methodology, Project administration, Writing-review and editing.

Funding: This study was co-financed at 85% by the European Union, European Regional Development Fund, and Regional Government of Extremadura (Junta de Extremadura). Managing Authority. Ministry of Finance. File number: GR24153.

Data Availability Statement: Data will be made available on request.

Acknowledgments: We gratefully acknowledge the financial support received from the Regional Government of Extremadura.

Conflicts of Interest: The authors declare that they have no known conflict of interest or personal relationships that could have appeared to influence in the collection, analysis or interpretation of the data, in the writing of the manuscript, or in the decision to publish the results the work reported in this paper.

References

1. Smith, R.A.H.; Bradshaw, A.D. The Use of Metal Tolerant Plant Populations for the Reclamation of Metalliferous Wastes. *Journal of Applied Ecology* **1979**, *16*, 595–612, doi:10.2307/2402534.
2. Sun, Z.; Hu, Y.; Cheng, H. Public Health Risk of Toxic Metal(Loid) Pollution to the Population Living near an Abandoned Small-Scale Polymetallic Mine. *Science of The Total Environment* **2020**, *718*, 137434, doi:10.1016/j.scitotenv.2020.137434.
3. Eurostat Objetivos de Desarrollo Sostenible Available online: https://ec.europa.eu/commission/presscorner/detail/es/ip_23_2887 (accessed on 8 July 2025).
4. González-Morales, M.; Rodríguez-González, M.Á.; Fernández-Pozo, L. Status of Ecosystem Services in Abandoned Mining Areas in the Iberian Peninsula: Management Proposal. *Toxics* **2023**, *11*, 275, doi:10.3390/toxics11030275.
5. González-Morales, M.; Fernández-Pozo, L.; Rodríguez-González, M.Á. Threats of Metal Mining on Ecosystem Services. Conservation Proposals. *Environmental Research* **2022**, *214*, 114036, doi:10.1016/j.envres.2022.114036.
6. Oropesa, A.-L.; Gala, J.-A.; Fernandez-Pozo, L.; Cabezas, J.; Soler, F. Lead Content in Soils and Native Plants near an Abandoned Mine in a Protected Area of South-Western Spain: An Approach to Determining the Environmental Risk to Wildlife and Livestock. *Environ Sci Pollut Res* **2019**, *26*, 30386–30398, doi:10.1007/s11356-019-06197-5.
7. Palma, P.; López-Orozco, R.; Mourinha, C.; Oropesa, A.L.; Novais, M.H.; Alvarenga, P. Assessment of the Environmental Impact of an Abandoned Mine Using an Integrative Approach: A Case-Study of the "Las

 doi:10.20944/preprints202603.1522.v1

Musas" Mine (Extremadura, Spain). *Science of The Total Environment* **2019**, *659*, 84–94, doi:10.1016/j.scitotenv.2018.12.321.

8. Madouh, T.A. Eco-Physiological Responses of Native Desert Plant Species to Drought and Nutritional Levels: Case of Kuwait. *Front. Environ. Sci.* **2022**, *10*, doi:10.3389/fenvs.2022.785517.
9. Díaz, O.G.E.; Fiegehen, L.E.G.; Guajardo, D.C.; Aguayo, S.N. Condicionantes de la retención estudiantil en "escuelas de segunda oportunidad" en Chile. *Revista Latinoamericana de Ciencias Sociales, Niñez y Juventud* **2019**, *17*, 1–27, doi:10.11600/1692715x.17201.
10. Kumar Rai, P.; Singh, J.S. Invasive Alien Plant Species: Their Impact on Environment, Ecosystem Services and Human Health. *Ecological Indicators* **2020**, *111*, 106020, doi:10.1016/j.ecolind.2019.106020.
11. Mishra, B.; Chandra, M. Evaluation of Phytoremediation Potential of Aromatic Plants: A Systematic Review. *Journal of Applied Research on Medicinal and Aromatic Plants* **2022**, *31*, 100405, doi:10.1016/j.jarmap.2022.100405.
12. Ez zoubi, Y.; Bousta, D.; Farah, A. A Phytopharmacological Review of a Mediterranean Plant: Lavandula Stoechas L. *Clinical Phytoscience* **2020**, *6*, 9, doi:10.1186/s40816-019-0142-y.
13. Carrasco, A.; Ortiz-Ruiz, V.; Martinez-Gutierrez, R.; Tomas, V.; Tudela, J. *Lavandula Stoechas* Essential Oil from Spain: Aromatic Profile Determined by Gas Chromatography–Mass Spectrometry, Antioxidant and Lipoxygenase Inhibitory Bioactivities. *Industrial Crops and Products* **2015**, *73*, 16–27, doi:10.1016/j.indcrop.2015.03.088.
14. Domingues, J.; Delgado, F.; Gonçalves, J.C.; Zuzarte, M.; Duarte, A.P. Mediterranean Lavenders from Section Stoechas: An Undervalued Source of Secondary Metabolites with Pharmacological Potential. *Metabolites* **2023**, *13*, 337, doi:10.3390/metabo13030337.
15. Dragićević, A.; Pavlović, D.; Tasić-Kostov, M. Hydrolates as Water Phase in Cosmetic Creams: Physicochemical and in Vivo Assessment. *Maced. Pharm. Bull.* **2023**, *69*, 125–126, doi:10.33320/maced.pharm.bull.2023.69.03.061.
16. Neves, J.M.; Matos, C.; Moutinho, C.; Queiroz, G.; Gomes, L.R. Ethnopharmacological Notes about Ancient Uses of Medicinal Plants in Trás-Os-Montes (Northern of Portugal). *Journal of Ethnopharmacology* **2009**, *124*, 270–283, doi:10.1016/j.jep.2009.04.041.
17. Livia, W.P.; Plata, Y.; Diaz, W.S.G. Disminución de pasivos ambientales mineros PAM mediante la obtención de espuma de vidrio. *Revista Colombiana de Materiales* **2021**, 9–9, doi:10.17533/RCM/udea.rcm.n18a03.
18. Lv, X.; Shen, W.; Wang, L.; Dong, Y.; Zhang, J.; Xie, Z. A Comparative Study on the Practical Utilization of Iron Tailings as a Complete Replacement of Normal Aggregates in Dam Concrete with Different Gradation. *Journal of Cleaner Production* **2019**, *211*, 704–715, doi:10.1016/j.jclepro.2018.11.107.
19. Geng, Y.; Cui, D.; Yang, L.; Xiong, Z.; Pavlostathis, S.G.; Shao, P.; Zhang, Y.; Luo, X.; Luo, S. Resourceful Treatment of Harsh High-Nitrogen Rare Earth Element Tailings (REEs) Wastewater by Carbonate Activated *Chlorococcum* Sp. Microalgae. *Journal of Hazardous Materials* **2022**, *423*, 127000, doi:10.1016/j.jhazmat.2021.127000.
20. Zhang, T.; Wang, L.; Zhang, Y. *Ekoloji*. 2018, pp. 1615–1624.
21. Zamarreño, R.; Díaz, F. Recuperación de metales económicamente importantes desde relaves mineros abandonados, usando biolixiviación en columnas de fase inversa, de bajo costo y ambientalmente sostenible. *Avances en Ciencias e Ingeniería* **2021**, *12*, 31–42.
22. Álvarez-Ayuso, E.; Murciego, A.; Rodríguez, M.A.; Mosser-Ruck, R. Cement Encapsulation Processes to Mitigate the Risks Posed by Different Types of Antimony-Bearing Mine Waste. *Journal of Cleaner Production* **2022**, *372*, 133671, doi:10.1016/j.jclepro.2022.133671.
23. Kinnunen, P.; Karhu, M.; Yli-Rantala, E.; Kivikytö-Reponen, P.; Mäkinen, J. A Review of Circular Economy Strategies for Mine Tailings. *Cleaner Engineering and Technology* **2022**, *8*, 100499, doi:10.1016/j.clet.2022.100499.
24. Kuppens, T.; Van Dael, M.; Vanreppelen, K.; Thewys, T.; Yperman, J.; Carleer, R.; Schreurs, S.; Van Passel, S. Techno-Economic Assessment of Fast Pyrolysis for the Valorization of Short Rotation Coppice Cultivated for Phytoextraction. *Journal of Cleaner Production* **2015**, *88*, 336–344, doi:10.1016/j.jclepro.2014.07.023.

 doi:10.20944/preprints202603.1522.v1

25. Qian, K.; Kumar, A.; Zhang, H.; Bellmer, D.; Huhnke, R. Recent Advances in Utilization of Biochar. *Renewable and Sustainable Energy Reviews* **2015**, *42*, 1055–1064, doi:https://doi.org/10.1016/j.rser.2014.10.074.
26. Kang, Z.; Xu, D.; Zhao, L.; Liu, D. Boosting Supercapacitor Performance with High-Specific Surface Area Porous Carbon Derived from Sugarcane Bagasse. *Journal of Energy Storage* **2024**, *104*, 114718, doi:10.1016/j.est.2024.114718.
27. Almada, I. Electrodos Para Supercondensadores Obtenidos Por Electrofdeposición, Universidad Autonoma de Madrid, 2015.
28. Norouzi, O.; Maria, F.D.; Dutta, A. Biochar-Based Composites as Electrode Active Materials in Hybrid Supercapacitors with Particular Focus on Surface Topography and Morphology. *Journal of Energy Storage* **2020**, *29*, 101291, doi:https://doi.org/10.1016/j.est.2020.101291.
29. Rawat, S.; Boobalan, T.; Krishna, B.B.; Sathish, M.; Hotha, S.; Bhaskar, T. Biochar for Supercapacitor Application: A Comparative Study. *Chemistry – An Asian Journal* **2022**, *17*, e202200982, doi:https://doi.org/10.1002/asia.202200982.
30. Andrade, M. das G.; da Boa Morte, E.S.; Batista dos Santos, D.C.M.; Castro, J.T.; Barbosa, J.T.P.; Teixeira, A.P.; Fernandes, A.P.; Welz, B.; dos Santos, W.P.C.; Nunes dos Santos, E.B.G.; et al. Sample Preparation for the Determination of Metals in Food Samples Using Spectroanalytical Methods—A Review. *Applied Spectroscopy Reviews* **2008**, *43*, 67–92, doi:10.1080/05704920701723980.
31. Palacios, O.F.; Zúñiga, L.E. Extracción del aceite esencial de Lavanda (lavándula angustifolia), mediante la metodología de arrastre de vapor. Trabajo Fin de Estudios (Ecuador). *Trabajo Fin de Estudios. Universidad Ecuador* **2022**.
32. Nazem, V.; Sabzalian, M.R.; Saeidi, G.; Rahimmalek, M. Essential Oil Yield and Composition and Secondary Metabolites in Self- and Open-Pollinated Populations of Mint *(Mentha* Spp.). *Industrial Crops and Products* **2019**, *130*, 332–340, doi:10.1016/j.indcrop.2018.12.018.
33. Hossain, M.A.; Piyatida, P.; da Silva, J.A.T.; Fujita, M. Molecular Mechanism of Heavy Metal Toxicity and Tolerance in Plants: Central Role of Glutathione in Detoxification of Reactive Oxygen Species and Methylglyoxal and in Heavy Metal Chelation. *Journal of Botany* **2012**, *2012*, 872875, doi:10.1155/2012/872875.
34. Srivastava, R.K.; Pandey, P.; Rajpoot, R.; Rani, A.; Dubey, R.S. Cadmium and Lead Interactive Effects on Oxidative Stress and Antioxidative Responses in Rice Seedlings. *Protoplasma* **2014**, *251*, 1047–1065, doi:10.1007/s00709-014-0614-3.
35. Garrido, I.; Ortega, A.; Hernández, M.; Fernández-Pozo, L.; Cabezas, J.; Espinosa, F. Effect of Antimony in Soils of an Sb Mine on the Photosynthetic Pigments and Antioxidant System of Dittrichia Viscosa Leaves. *Environ Geochem Health* **2021**, *43*, 1367–1383, doi:10.1007/s10653-020-00616-0.
36. Sierra, M.J.; Millán, R.; Esteban, E. Mercury Uptake and Distribution in *Lavandula Stoechas* Plants Grown in Soil from Almadén Mining District (Spain). *Food and Chemical Toxicology* **2009**, *47*, 2761–2767, doi:10.1016/j.fct.2009.08.008.
37. Arenas-Lago, D.; Carvalho, L.C.; Santos, E.S.; Abreu, M.M. Influence of Seed Source and Soil Contamination on Ecophysiological Responses of Lavandula Pedunculata in Rehabilitation of Mining Areas. *Plants* **2022**, *11*, 105, doi:10.3390/plants11010105.
38. Çolak, S.; Yilmaz, Ş.B.A.; Öztekin, E. Bioaccumulation Factors of Heavy Metal(Loid)s in Some Medicinal and Aromatic Plants Species: Example of Zonguldak/Türkiye. *Water Air Soil Pollut* **2023**, *234*, 522, doi:10.1007/s11270-023-06536-w.
39. Angelova, V.R.; Grekov, D.F.; Kisyov, V.K.; Ivanov, K.I. Potential of Lavender (Lavandula Vera L.) for Phytoremediation of Soils Contaminated with Heavy Metals. *International J. of Agricultural and Biosystems Engineering* **2015**, *9*.
40. Bella, S.L.; Tuttolomondo, T.; Dugo, G.; Ruberto, G.; Leto, C.; Napoli, E.M.; Potortì, A.G.; Fede, M.R.; Virga, G.; Leone, R.; et al. Composition and Variability of the Essential Oil of the Flowers of Lavandula Stoechas from Various Geographical Sources. *Natural Product Communications* **2015**, *10*, 1934578X1501001150, doi:10.1177/1934578X1501001150.
41. Şahinler, S.Ş.; Yılmaz, B.S.; Sarıkürkcü, C.; Tepe, B. The Importance of Lavandula Stoechas L. in Pharmacognosy and Phytotherapy. *Int. J. Sec. Metabolite* **2022**, *9*, 360–376, doi:10.21448/ijsm.1098975.

 doi:10.20944/preprints202603.1522.v1

42. Rufino, A.T.; Ribeiro, M.; Sousa, C.; Judas, F.; Salgueiro, L.; Cavaleiro, C.; Mendes, A.F. Evaluation of the Anti-Inflammatory, Anti-Catabolic and pro-Anabolic Effects of *E*-Caryophyllene, Myrcene and Limonene in a Cell Model of Osteoarthritis. *European Journal of Pharmacology* **2015**, *750*, 141–150, doi:10.1016/j.ejphar.2015.01.018.
43. Sharma, M.; Grewal, K.; Jandrotia, R.; Batish, D.R.; Singh, H.P.; Kohli, R.K. Essential Oils as Anticancer Agents: Potential Role in Malignancies, Drug Delivery Mechanisms, and Immune System Enhancement. *Biomedicine & Pharmacotherapy* **2022**, *146*, 112514, doi:10.1016/j.biopha.2021.112514.
44. Reyes-Jurado, F.; Navarro-Cruz, A.R.; Ochoa-Velasco, C.E.; Palou, E.; López-Malo, A.; Ávila-Sosa, R. Essential Oils in Vapor Phase as Alternative Antimicrobials: A Review. *Crit Rev Food Sci Nutr* **2020**, *60*, 1641–1650, doi:10.1080/10408398.2019.1586641.
45. Blažeković, B.; Vladimir-Knežević, S.; Brantner, A.; Štefan, M.B. Evaluation of Antioxidant Potential of Lavandula x Intermedia Emeric Ex Loisel. "Budrovka": A Comparative Study with L. Angustifolia Mill. *Molecules* **2010**, *15*, 5971–5987, doi:10.3390/molecules15095971.
46. Di Sotto, A.; Mazzanti, G.; Carbone, F.; Hrelia, P.; Maffei, F. Genotoxicity of Lavender Oil, Linalyl Acetate, and Linalool on Human Lymphocytes in Vitro. *Environmental and Molecular Mutagenesis* **2011**, *52*, 69–71, doi:10.1002/em.20587.
47. Zheljazkov, V.D.; Craker, L.E.; Xing, B. Effects of Cd, Pb, and Cu on Growth and Essential Oil Contents in Dill, Peppermint, and Basil. *Environmental and Experimental Botany* **2006**, *58*, 9–16, doi:10.1016/j.envexpbot.2005.06.008.
48. Gautam, M.; Agrawal, M. Influence of Metals on Essential Oil Content and Composition of Lemongrass (*Cymbopogon Citratus* (D.C.) Stapf.) Grown under Different Levels of Red Mud in Sewage Sludge Amended Soil. *Chemosphere* **2017**, *175*, 315–322, doi:10.1016/j.chemosphere.2017.02.065.
49. Gonzalez-Rivera, J.; Campanella, B.; Pulidori, E.; Bramanti, E.; Tiné, M.R.; Bernazzani, L.; Onor, M.; Bàrberi, P.; Duce, C.; Ferrari, C. From Volatiles to Solid Wastes: Towards the Full Valorization of Lavender and Rosemary by Simultaneous in Situ Microwaves and Ultrasounds Irradiation Extraction. *Industrial Crops and Products* **2023**, *194*, 116362, doi:10.1016/j.indcrop.2023.116362.
50. Thommes, M.; Kaneko, K.; Neimark, A.V.; Olivier, J.P.; Rodriguez-Reinoso, F.; Rouquerol, J.; Sing, K.S.W. Physisorption of Gases, with Special Reference to the Evaluation of Surface Area and Pore Size Distribution (IUPAC Technical Report). *Pure and Applied Chemistry* **2015**, *87*, 1051–1069, doi:10.1515/pac-2014-1117.
51. Brunauer, S.; Emmett, P.H.; Teller, E. *Journal of the American Chemical Society*. 1938,.
52. Barret, E.P.; Joyner, L.G.; Halenda, P.P. *Journal of the American Chemical Society*. 1951,.
53. Li, S.; Chen, G. Thermogravimetric, Thermochemical, and Infrared Spectral Characterization of Feedstocks and Biochar Derived at Different Pyrolysis Temperatures. *Waste Management* **2018**, *78*, 198–207, doi:10.1016/j.wasman.2018.05.048.
54. Kawakami, M.; Kanba, H.; Sato, K.; Takenaka, T.; Gupta, S.; Chandratilleke, R.; Sahajwalla, V. Characterization of Thermal Annealing Effects on the Evolution of Coke Carbon Structure Using Raman Spectroscopy and X-Ray Diffraction. *ISIJ Int.* **2006**, *46*, 1165–1170, doi:10.2355/isijinternational.46.1165.
55. Chu, H.; Lu, Z.; Man, M.; Song, S.; Zhang, H.; Cheng, J.; Zhao, X.; Duan, J.; Chen, X.; Zhu, Y. Hard Carbon-Based Electrode Boosts the Performance of a Solid-State Symmetric Supercapacitor. *Journal of Energy Storage* **2024**, *76*, 109660, doi:10.1016/j.est.2023.109660.
56. Barroso Bogeat, A. Understanding and Tuning the Electrical Conductivity of Activated Carbon: A State-of-the-Art Review. *Critical Reviews in Solid State and Materials Sciences* **2021**, *46*, 1–37, doi:10.1080/10408436.2019.1671800.
57. Moliner, R. *Bol Grupo Español del Carbón*. 2016,.
58. Eliad, L.; Pollak, E.; Levy, N.; Salitra, G.; Soffer, A.; Aurbach, D. *Appl. Phys. A*. 2006,.
59. Jo, K.; Ha, J.; Ryu, J.; Lee, E.; Lee, H. DC 4-Point Measurement for Total Electrical Conductivity of SOFC Cathode Material. *Applied Sciences* **2021**, *11*, 4963, doi:10.3390/app11114963.

 doi:10.20944/preprints202603.1522.v1

disclaim responsibility for any injury to people or property resulting from any ideas, methods, instructions or products referred to in the content.